Soft Matter

PAPER

View Article Online
View Journal | View Issue

Cite this: *Soft Matter*, 2015, 11, 8253

Exceptionally tough and notch-insensitive magnetic hydrogels†

Hussain Haider,‡[ab] Can Hui Yang,‡[a] Wen Jiang Zheng,[ab] Jian Hai Yang,[ab] Mei Xiang Wang,[ab] Sen Yang,[b] Miklós Zrínyi,[c] Yoshihito Osada,[d] Zhigang Suo,[e] Qiqing Zhang,[f] Jinxiong Zhou*[a] and Yong Mei Chen*[ab]

Received 16th June 2015,
Accepted 27th August 2015

DOI: 10.1039/c5sm01487e

www.rsc.org/softmatter

Most existing magnetic hydrogels are weak and brittle. The development of strong and tough magnetic hydrogels would extend their applications into uncultivated areas, such as in actuators for soft machines and guided catheters for magnetic navigation systems, which is still a big challenge. Here a facile and versatile approach to fabricating highly stretchable, exceptionally tough and notch-insensitive magnetic hydrogels, Fe_3O_4@Fe-alginate/polyacrylamide (PAAm), is developed, by dispersing alginate-coated Fe_3O_4 nanoparticles into the interpenetrating polymer networks of alginate and PAAm, with hybrid physical and chemical crosslinks. A cantilever bending beam actuator as well as a proof-of-concept magnetically guided hydrogel catheter is demonstrated. The method proposed in this work can be integrated into other strong and tough magnetic hydrogels for the development of novel hydrogel nanocomposites with both desirable functionality and superior mechanical properties.

1. Introduction

As a representative soft intelligent material combining the properties of magnetism and viscoelasticity,[1–6] magnetic hydrogels have attracted intensive attention due to their unique features including biocompatibility, low friction, fast response, and spatial and temporal control manipulation, as well as non-invasive and remote actuation.[7–13] Unfortunately, most existing magnetic hydrogels are brittle and fragile.[14,15] Some magnetic hydrogels achieve good mechanical strength (~2 MPa tensile strength, and ~400% stretchability),[16] but these values are markedly decreased when the samples contain small cracks or notches. These hydrogels are very sensitive to notches, meaning they are not tough.[17] Mechanical weakness confines current magnetic hydrogels to limited low-level loading areas such as drug delivery and release,[18,19] hyperthermia cancer therapy,[20] 3D cell culture,[21] and enzyme immobilization.[22] By endowing magnetic hydrogels with superior mechanical properties, tough magnetic hydrogels are expected to lead to breakthrough applications beyond the horizons of current hydrogels, where toughness, stretchability and fault-tolerance are the first priorities. Examples include actuators or artificial muscles for soft robotics, pumps or valves for fluidic control, and switches for micro-machines, as well as magnetic catheters for remote magnetic manipulation systems.

In this contribution, we firstly propose a facile and versatile strategy to prepare a tough and notch-insensitive magnetic hydrogel, designated Fe_3O_4@Fe-alginate/PAAm, based on our previously developed hybrid crosslinked hydrogel.[23] This is realized by uniformly dispersing alginate-coated Fe_3O_4 nanoparticles into the interpenetrated polymer networks of alginate and PAAm. Alginate is one of the most abundant naturally derived polysaccharides possessing many favourable properties, such as gelation in mild conditions, controllable degradation, and excellent biocompatibility.[24] PAAm is a popular synthetic polymer with excellent flexibility, biocompatibility and hydrophilicity.[25,26] Coating alginate polymers on the surface of Fe_3O_4 nanoparticles is vital to achieve tough and notch-insensitive magnetic hydrogels. The coated alginate polymers have two functions, *i.e.*, uniformly dispersing the magnetic nanoparticles into the hydrogel matrix *via* electrostatic repulsion, and stabilizing the nanoparticles into the polymer networks *via* a physical interaction. It is noteworthy

[a] *State Key Laboratory for Strength and Vibration of Mechanical Structures, International Center for Applied Mechanics and School of Aerospace, Xi'an Jiaotong University, Xi'an 710049, China. E-mail: chenym@mail.xjtu.edu.cn, jxzhouxx@mail.xjtu.edu.cn*
[b] *School of Science, State Key Laboratory for Mechanical Behaviour of Materials, Collaborative Innovation Center of Suzhou Nano Science and Technology, Xi'an Jiaotong University, Xi'an, 710049, China*
[c] *Laboratory of Nanochemistry, Department of Biophysics and Radiation Biology, Semmelweis University, Nagyváradtér 4, H-1084 Budapest, Hungary*
[d] *RIKEN, 2-1, Hirosawa, Wako, Saitama 351-0198, Japan*
[e] *School of Engineering and Applied Science, Kavli Institute of Bionano Science and Technology, Harvard University, Cambridge, Massachusetts 02318, USA*
[f] *Institute of Biomedical Engineering, Chinese Academy of Medical Science & Peking Union Medical College, Tianjin, 300192, China*

† Electronic supplementary information (ESI) available: Fracture energy calculation, FTIR spectra, size distribution of nanoparticles, magnetic hysteresis loop, compression hysteresis curves, table of mechanical properties of the tough magnetic hydrogels and four movies. See DOI: 10.1039/c5sm01487e

‡ Hussain Haider and Can Hui Yang contributed equally to this work.

that besides the toughness exhibited by the high fracture energy ($\sim$2800 J m^{-2}), the magnetic hydrogels also demonstrate notch-insensitivity under $\sim$9 times stretch. A cantilever bending beam actuator and a proof-of-concept magnetically guided hydrogel catheter are also demonstrated to show their excellent mechanical and magnetic performances. The proposed facile strategy to achieve tough and notch-insensitive magnetic hydrogels can be adapted to other tough hydrogel systems, broadening the applications of soft smart materials across various frontiers.

2. Materials and methods

2.1 Materials

Sodium-alginate (Na-alginate) (viscosity: 300–500 mPa s) was purchased from Yantai Xinwang Haizao Co. Ltd (China). Acrylamide (AAm), ferric nitrate nonahydrate ($Fe(NO_3)_3{\cdot}9H_2O$), iron(II) chloride tetrahydrate ($FeCl_2{\cdot}4H_2O$) and iron(III) chloride hexahydrate ($FeCl_3{\cdot}6H_2O$) were obtained from Tianjin Fuchen (China). *N*,*N*′-Methylenebisacrylamide (MBAA) was purchased from Wolsen Co. Ltd (China), and ammonium peroxydisulphate (APS) was bought from Spectrum Co. Ltd (China). *N*,*N*,*N*′,*N*′-Tetramethylethylenediamine (TEMED) was purchased from Aladdin, Co. Ltd (China). All materials were used as received and all solutions were prepared in deionized water.

2.2 Synthesis of magnetic nanoparticles

Magnetic nanoparticles (Fe_3O_4) were synthesized by a coprecipitation method using Fe^{2+} and Fe^{3+} ions in basic medium. $FeCl_2{\cdot}4H_2O$ and $FeCl_3{\cdot}9H_2O$ (the molar ratio of Fe^{2+} to Fe^{3+} is 0.55 : 1) were dissolved in deionized water at 60 °C. The solution was adequately filtered to remove impurities. NaOH (5.0 M) was added into the solution to obtain black magnetic nanoparticles (pH = 14). In order to achieve homogeneous dispersion and stabilization of the nanoparticles in the hydrogel matrix, Fe_3O_4 nanoparticles were coated with alginate polymer as follows. An alginate solution (0.8 wt%) was added to the suspension of magnetic nanoparticles. The weight percentage of the alginate solution was 1.0 wt% with respect to the weight of the nanoparticles. Then the solution was heated and vigorously stirred simultaneously for 30 minutes at 60 °C, followed immediately by slow stirring for 1 h at 80 °C under a nitrogen atmosphere, resulting in a ferrofluid containing alginate-coated Fe_3O_4 (Fe_3O_4@Na-alginate) nanoparticles. To remove impurities that hinder the gelation of the magnetic hydrogel, the above ferrofluid was purified as follows. Firstly, the ferrofluid was washed with deionized water five times. Then, negatively charged poly(2-acrylamido-2-methyl propyl sulfonic acid) (PAMPS) hydrogel (see ESI† for details) was soaked in 2.0% ferrofluid (100 mL) to remove Fe^{2+} and Fe^{3+} for 2 days. In this process, Fe^{2+} and Fe^{3+} ions diffused from solution into the polymer network of the PAMPS hydrogel *via* an electrostatic interaction.[14] Then, the PAMPS hydrogel containing absorbed Fe^{2+} and Fe^{3+} was removed. After collection, the Fe_3O_4@Na-alginate nanoparticles were dried at 60 °C for 6 h. Fourier transform infrared (FTIR) spectroscopic analysis (BRUKER TENSOR 27, Bruker) was used to analyse the samples.

2.3 Synthesis of tough magnetic Fe_3O_4@Fe-alginate/PAAm hydrogels

We synthesized tough magnetic hydrogels by a two-step method. Firstly, the powder of AAm and Na-alginate (the weight ratio of AAm to Na-alginate is 8 : 1) were dissolved in the ferrofluid containing the alginate-coated Fe_3O_4 nanoparticles, in which the total amount of AAm and Na-alginate was 14 wt%. The weight percentage of alginate-coated Fe_3O_4 nanoparticles in the ferrofluid was 1.0, 2.0, 3.0, 4.0, 5.0, 10.0 and 20.0 wt%, with respect to the total weight of the polymers and water. The ferrofluid containing the alginate-coated Fe_3O_4 nanoparticles, alginate polymers and AAm monomer was carefully stirred for 1 hour, resulting in a homogeneous suspension. After this, a crosslinking agent (MBAA) (0.028 mol%), a thermo-initiator (APS) (0.031 mol%) and an accelerator (TEMED) (0.152 mol%) were dissolved into the suspension. The suspension was transferred into a glass mould and kept at 25 °C for 20 h to remove bubbles. Then the mould was placed in a water bath at 50 °C for 6 h for gelation. This step produced the Fe_3O_4@Na-alginate/PAAm hydrogel. The resulting Fe_3O_4@Na-alginate/PAAm hydrogel was separated from the mould and soaked in an aqueous solution of 0.3 M $Fe(NO_3)_3$ for 6 h at room temperature. In this step, Fe^{3+} ions in the external solution diffused into the hydrogel and crosslinked alginate, resulting in the tough Fe_3O_4@Fe-alginate/PAAm hydrogel. We immersed the Fe_3O_4@Fe-alginate/PAAm hydrogel in the aqueous solution of 0.3 M $Fe(NO_3)_3$ for as long as 6 hours to avoid gradient crosslinks; this was supported by the observation of excellent mechanical properties. The following equation[27] was used to estimate the soaking time of the sample in the aqueous solution:

$$t = \frac{4}{\pi^2}\frac{H^2}{D}$$

where H is half of the thickness and D is the diffusion coefficient. The soaking time is prolonged with an increase in the sample thickness and *vice versa*. For example, in the case of our samples where the thickness is 2 mm and $D = 6.04 \times 10^{-4}$ mm^2 s^{-1},[28] then an approximate time of $\sim$0.0972 h is obtained. Thus, a 6 h soaking time is much longer than the estimated time to guarantee a complete ion-exchange and gelation. In fact, the crosslinking of alginate through Fe^{3+} cation diffusion barely changed with sample size because our samples are relatively thin and are immersed in the solution of Fe^{3+} ions for a long enough time. So the samples were homogeneous with excellent mechanical properties as supported by the experimental results.

2.4 Scanning electron microscopy (SEM) and transmission electron microscopy (TEM) analysis

The size and morphology of the Fe_3O_4 nanoparticles embedded in the Fe_3O_4@Fe-alginate/PAAm hydrogels were observed using field emission scanning electron microscopy (FE-SEM) (JEOLJSM-7000F). The Fe_3O_4@Fe-alginate/PAAm hydrogels were freeze-dried in a vacuum freeze-dryer (Hetopower dry LL1500, Thermo, USA) for 12 h.

TEM (JEOL JEM-2100) operating at an accelerating voltage of 200 kV was also used to analyze the magnetic hydrogels. After the freeze-dried magnetic hydrogel sample was ground and dispersed in ethanol using an ultrasonic bath, droplets of this suspension were transferred onto a carbon-coated grid and dried in air before TEM analysis.

2.5 Mechanical characterization

Tensile and compressive tests of the Fe_3O_4@Fe-alginate/PAAm hydrogels were performed using a testing machine (CMT6503, MTS, USA) with a 500 N load cell for tension and 5000 N for compression. The samples for tension were cut into a dumbbell shape with length 35 mm, width 2 mm and gauge length 12 mm, while those for compression were cylinder-shaped with a height of 4 mm and a diameter of 12 mm.

The sizes of the samples were measured using a caliper (Digimatic Caliper, Hengliang Liangju Co. Ltd, Shanghai, China). The strain rate (50, 100, 250 mm min^{-1}) negligibly affects the hysteresis of tension or compression. In the process of the mechanical tests, creep and water loss are major concerns for data accuracy. Therefore, we use a relatively high strain rate of 100 mm min^{-1} because our magnetic hydrogels are very stretchable. In addition, avoiding water evaporation and time consumption are also concerns. The constant velocity of the crosshead was 1 mm min^{-1} for the compressive tests. The abrupt drop of the load in the unloading compression process in the stress–strain curves is due to the machine halting. The measurement and calculation of the fracture energy of the Fe_3O_4@Fe-alginate/PAAm hydrogels are described in the ESI,† Fig. S1.

2.6 Magnetic characterization

The magnetic properties of the dehydrated Fe_3O_4@Fe-alginate/PAAm hydrogels and the Fe_3O_4 nanoparticles were investigated

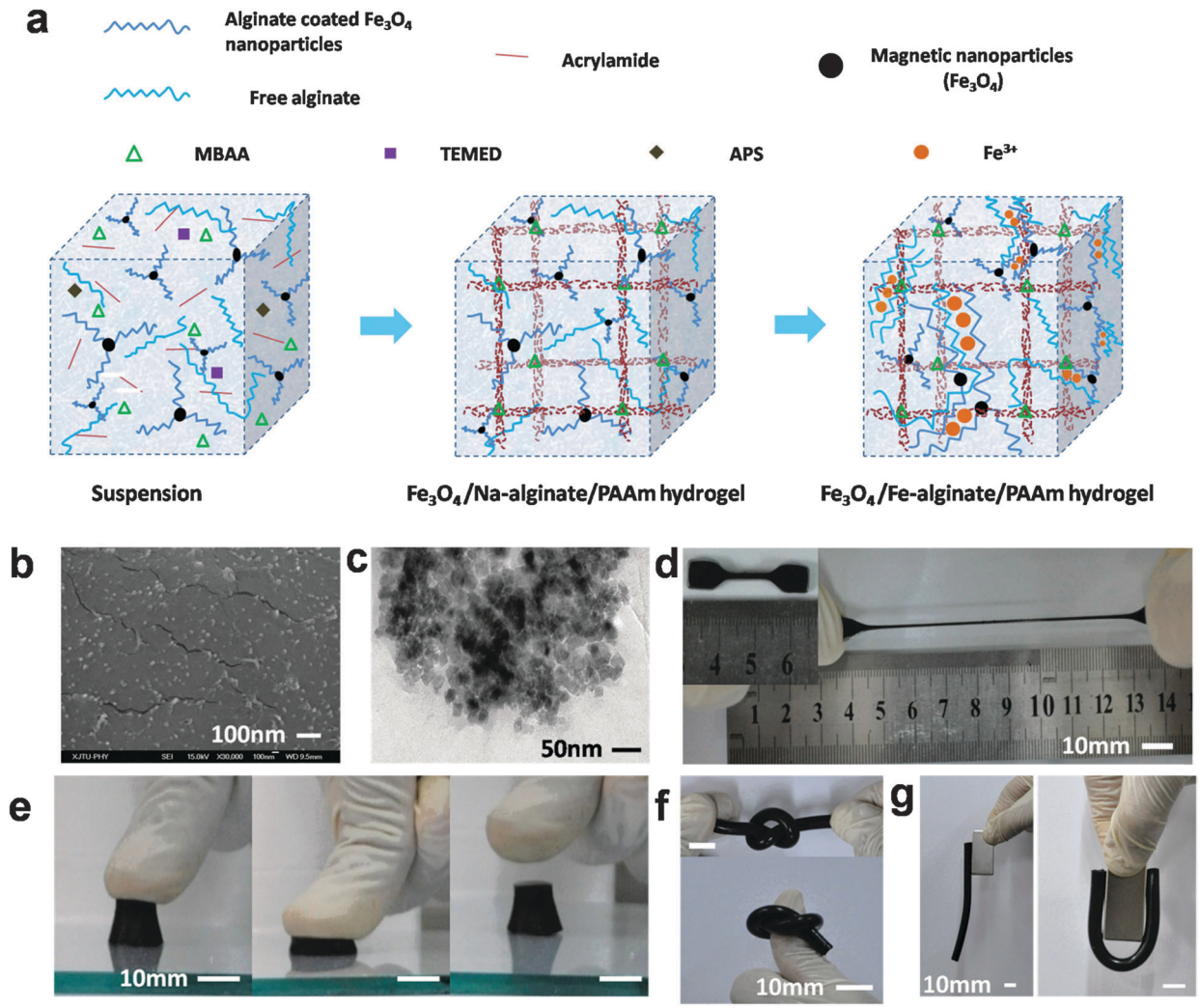

Fig. 1 Preparation process, SEM and TEM images and photographs of the tough magnetic Fe_3O_4@Fe-alginate/PAAm hydrogels. (a) Schematic process of the preparation of the magnetic hydrogel. (b) SEM and (c) TEM images of the Fe_3O_4 nanoparticles embedded in the magnetic hydrogel. The Fe_3O_4@Fe-alginate/PAAm hydrogel is strong and tough enough to undergo (d) extensive stretching, (e) compression, (f) knotting and twisting, and (g) shows a magnetic response to magnetic attraction. The weight content of Fe_3O_4 nanoparticles in the magnetic hydrogels is 5.0 wt% for (a), (c–g) and 1.0 wt% for (b).

using a vibrating sample magnetometer (735 VSM Controller, LakeShore) with a maximum applied magnetic field of 9000 Oe at room temperature.

3. Results and discussion

3.1 Preparation of tough magnetic hydrogels

The design strategy is important for obtaining our tough and notch-insensitive Fe_3O_4@Fe-alginate/PAAm magnetic hydrogels. We developed a facile and feasible procedure as follows (Fig. 1a). Firstly, to homogeneously disperse and stabilize the Fe_3O_4 nanoparticles into the hydrogel matrix, Fe_3O_4@Na-alginate nanoparticles were prepared. FTIR analysis confirmed the existence of alginate in the modified Fe_3O_4 nanoparticles. The bands of the carboxylic groups (COO^-) (1626 cm^{-1}, 1387 cm^{-1}) of alginate and the band of Fe–O (584 cm^{-1}) of Fe_3O_4 are present in the spectrum of Fe_3O_4@Na-alginate (ESI,† Fig. S2).[29] This indicates that the Fe_3O_4 nanoparticles are well decorated with alginate polymers. Secondly, Fe_3O_4@Na-alginate/PAAm hydrogels were prepared by dissolving polymer (Na-alginate), monomer (AAm), covalent crosslinker (MBAA), thermo-initiator (APS) and accelerator (TEMED) into the suspension of Fe_3O_4@Na-alginate nanoparticles and gelating the suspension into a glass mould at 50 °C for 6 h. By controlling the weight content of the Fe_3O_4@Na-alginate nanoparticles ($W_{Fe_3O_4}$) in a reasonable range of 1–20 wt%, homogeneous Fe_3O_4@Na-alginate/PAAm hydrogels can be obtained, whereas complete gelation and polymerization of AAm is hard to achieve when $W_{Fe_3O_4} > 20$ wt%. In the obtained Fe_3O_4@Na-alginate/PAAm hydrogel, only PAAm was loosely crosslinked by covalent bonds, while non-crosslinked Na-alginate polymer chains and Fe_3O_4@Na-alginate nanoparticles were thoroughly dispersed into and interweaved with the PAAm polymer networks.

Finally, tough Fe_3O_4@Fe-alginate/PAAm hydrogels were fabricated by immersing the Fe_3O_4@Na-alginate/PAAm hydrogels in $Fe(NO_3)_3$ solution. In this process, Fe^{3+} cations diffuse from the external bulk solution into the interior polymer networks of the Fe_3O_4@Na-alginate/PAAm hydrogels, replace the Na^+ cations, and crosslink alginate polymers to form the tough and notch-insensitive magnetic Fe_3O_4@Fe-alginate/PAAm hydrogels. Both free-alginate polymer chains and the alginate polymer chains attached onto the surface of Fe_3O_4 nanoparticles were crosslinked by trivalent Fe^{3+} cations *via* the formation of a $Fe(COO)_3$ coordination compound,[30] leading to a 3D polymer network.

SEM (Fig. 1b) and TEM (Fig. 1c) images show that the Fe_3O_4 nanoparticles (~20 nm diameter) (ESI,† Fig. S3) are well dispersed within the hydrogel matrix. The cracks on the surface of the magnetic hydrogel are observed in the SEM image because they are formed during the process of preparing the freeze-dried samples (Fig. 1b).

The magnetic Fe_3O_4@Fe-alginate/PAAm hydrogel is mechanically robust (Fig. 1d–f) and exhibits excellent magnetic properties (Fig. 1g). To further demonstrate its magnetic response, a magnetic hydrogel rod (length 10 mm, diameter 6 mm) was driven by a NdFeB alloy permanent magnet. The hydrogel swam quickly in water under magnetic guidance (Movie S1 in the

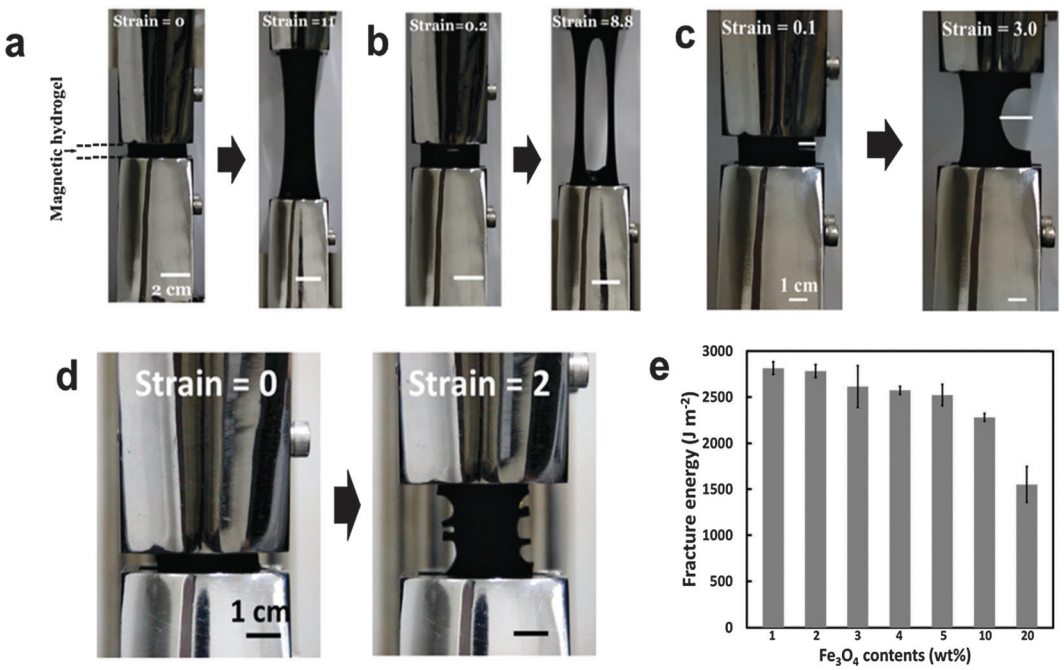

Fig. 2 The magnetic hydrogel is highly stretchable, tough and notch-insensitive. (a) A strip of undeformed magnetic hydrogel (5.0 wt%) was fixed to two clamps and then stretched to 11.0 times its initial length without rupturing. (b) A horizontal notch was cut into the middle of the magnetic hydrogel using a razor blade, and the notched magnetic hydrogel was stretched to 8.8 times its original length. A small strain of 0.2 was used to make the pre-existing notch clearly visible initially. The notch tips became blunt due to large deformation but the hydrogel did not rupture. (c) A sample with a side edge notch and (d) multiple notches were able to sustain large deformation, without merging of the adjacent notches. (e) Fracture energy of the magnetic hydrogels with various Fe_3O_4 nanoparticle contents. Error bars denote the standard deviation from at least three experiments.

ESI†). The generic strategy of fabricating a tough and notch-insensitive magnetic hydrogel can potentially be adapted to other strong hydrogel systems, and is also easy to be scaled up for mass production which is important for realizing their practical applications.

3.2 Mechanical properties of tough magnetic hydrogels

Interestingly, a notch-insensitive performance was found for the Fe_3O_4@Fe-alginate/PAAm hydrogels containing 1–5 wt% magnetic nanoparticles. As a typical example, a 30 × 35 × 2 mm^3 Fe_3O_4@Fe-alginate/PAAm hydrogel ($W_{Fe_3O_4}$ = 5.0 wt%) strip can be stretched to 11 times its original length without rupturing (Fig. 2a). The same sample, pre-cracked with a 10 mm central crack, can be stretched up to 8.8 times its original length. Even being subjected to such a large elongation, the crack just became blunt without rupturing (Fig. 2b). To further demonstrate the notch-insensitivity, a magnetic hydrogel of the same dimensions with an edge notch (length 1 cm) was elongated to a large stretch. It also exhibited extreme notch-insensitivity and high toughness. After being stretched to strain 3 and then unloaded to zero force, the sample maintained its original shape well with negligible residual strain except for a small propagation of the notch (Fig. 2c and Movie S2 in the ESI†). Similarly, the same sample symmetrically cut with multiple cracks at both sides (0.5 mm length separated by 2 mm distance) can also sustain a large stretch. The adjacent notches did not merge together at 2 strain (Fig. 2d), or even at 3 strain (Movie S3 in the ESI†).

Fig. 3 and 4 explain the tensile and compressive mechanical properties of the magnetic hydrogels when the content of Fe_3O_4 magnetic nanoparticles is varied from 1.0–20.0 wt%. We want to make it clear that the stress used in the tensile and compression tests is nominal stress. Note that in our experiments the stress mentioned is nominal stress and strain is used to describe a large deformation. The experimental results are summarized in Table S1 (ESI†). It should be pointed out that a distinct yielding phenomenon was observed for the tensile tests of all samples (Fig. 3a). This is often a characteristic feature of tough hydrogels,[23] but is seldom observed in magnetic hydrogels. The tensile results indicate that the maximum strain and tensile strength greatly depend on the content of Fe_3O_4 nanoparticles (Fig. 3a), while the measured tensile modulus does not, staying at ~200 kPa (Fig. 3b). Choosing the hydrogels containing 1.0 and 20.0 wt% Fe_3O_4 nanoparticles as two typical examples, the results are: 11.4 ± 1.5 rupture tensile strain and 0.915 ± 0.053 MPa tensile strength for the 1.0 wt% sample, and 2.7 ± 0.4 and 0.201 ± 0.009 MPa for the 20.0 wt% sample. The magnetic hydrogels also exhibit excellent compression properties (Fig. 4). The hydrogels can recover to their original shape without breaking after 90% compression (Fig. 4a), giving compressive strengths as high as

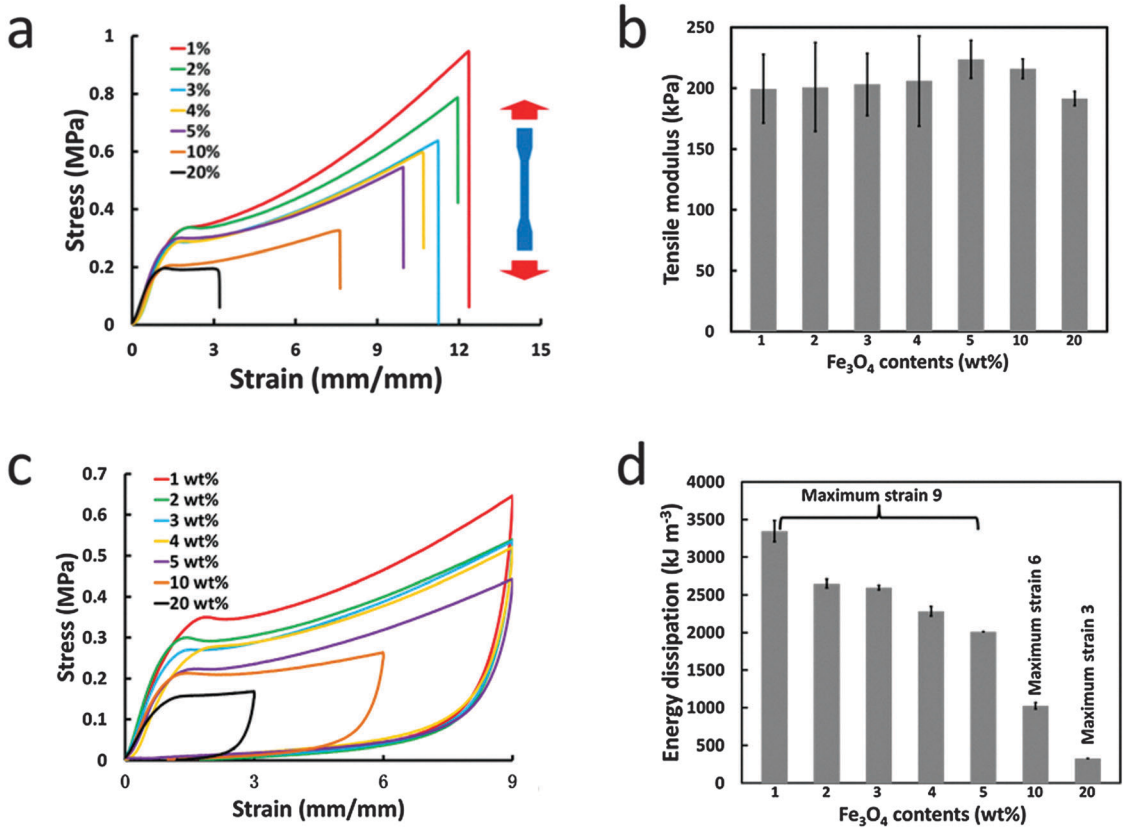

Fig. 3 Tensile mechanical properties of the tough magnetic hydrogels: (a) tensile stress–strain curves, (b) tensile modulus, (c) tensile hysteresis curves, and (d) energy dissipation of the magnetic hydrogels with varying Fe_3O_4 nanoparticle content. Dumbbell-shaped samples were employed to conduct the experiments. Error bars denote the standard deviation from at least three experiments.

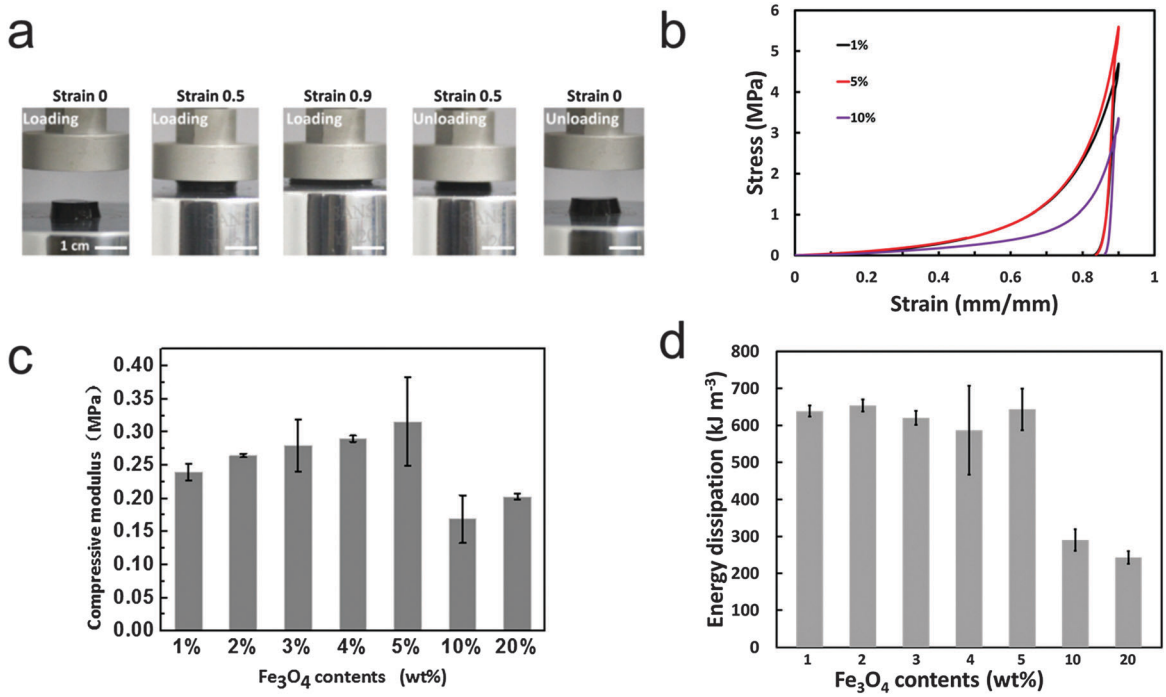

Fig. 4 Compressive mechanical properties of the tough magnetic hydrogels: (a) photographs of the compression process of the magnetic hydrogel ($W_{Fe_3O_4}$ = 5.0 wt%). The sample was first compressed to a maximum strain of 0.9, and then unloaded to zero. The hydrogel almost retained its original state after unloading. (b) Compressive hysteresis curves, (c) compressive modulus, and (d) energy dissipation of the magnetic hydrogels with different weight content of Fe_3O_4 nanoparticles. Error bars denote the standard deviation from at least three experiments.

3.1 ± 0.2–5.6 ± 0.6 MPa (Fig. 4b) and ~200 kPa compressive modulus (Fig. 4c) over the range from 1.0–20.0 wt%.

Hysteresis curves are used to describe the energy dissipating capability of magnetic hydrogels which characterizes their toughness. Fig. 3c and 4b describe the hysteresis tests for tension and compression, respectively. The maximum strain was fixed at 90% for compression (Fig. 4b) but varied for tension, specifically, 900% for the 1.0, 2.0, 3.0, 4.0 and 5.0 wt% samples, 600% for the 10.0 wt% sample and 300% for the 20.0 wt% sample (Fig. 3c). To provide a clear graph for compression, only the curves of the 1.0, 5.0 and 10.0 wt% samples are selected (Fig. 4b). The remaining curves of the 2.0, 3.0, 4.0 and 20.0 wt% samples are shown in Fig. S4 (ESI†).

The area enclosed by each loading–unloading curve gives the corresponding energy dissipation of the cycle. The results are presented in Fig. 3d and 4d for the tensile and compressive tests, respectively. For the samples with $W_{Fe_3O_4} < 5\%$, the tensile tests exhibit energy dissipations as high as ~2300–3400 kJ m^{-3} (Fig. 3d), and the compressive tests give ~650 kJ m^{-3} (Fig. 4d).

To quantitatively characterize the toughness of the magnetic hydrogels, we follow the well-established procedure to measure the fracture energy of the hydrogels (ESI,† Fig. S1). Although the fracture energy decreases with increasing $W_{Fe_3O_4}$, it falls into the range of 1550.5 ± 194.9–2814.0 ± 69.6 J m^{-2} (Fig. 2e). The fracture energy of the magnetic hydrogel reported herein is comparable to cartilage and common rubber (~1000 J m^{-2}),[31,32] and should be enough for many applications.

The tendency of the mechanical performance to decrease with an increasing amount of magnetic nanoparticles is understood as follows. Embedding magnetic nanoparticles into the polymer networks introduces plenty of interfaces between rigid particles and soft polymers, resulting in a heterogeneous system. These interfaces are weak and responsible for the failure of hydrogel composites. When an external load is applied, the heterogeneity causes stress concentration and leads to hydrogel damage, especially for the samples with a high nanoparticle content. Thus, as the content of Fe_3O_4 nanoparticles increases, both the tensile strength and tensile strain decrease. A similar trend is observed in polyvinyl alcohol (PVA) based magnetic hydrogels containing carbonyl iron particles, in which a high nanoparticle content deteriorates the tensile properties of the magnetic hydrogel.[33]

Although somewhat of a decrease in fracture energy was found due to the embedment of a large amount of alginate-coated Fe_3O_4 nanoparticles, the current reported magnetic hydrogels still exhibit excellent mechanical properties.

3.3 Cantilever bending beam actuator

To explore the possibility of using the magnetic hydrogels as soft actuators, we designed and conducted a magnetic response experiment of a cantilever bending beam actuator (Fig. 5). A cylinder-shaped cantilever beam, 100 mm in length and 6 mm in diameter, was activated by a permanent NdFeB alloy magnet. The tip-titled displacement and the radius of curvature were measured (Fig. 5a). The tip-tilted displacement is determined

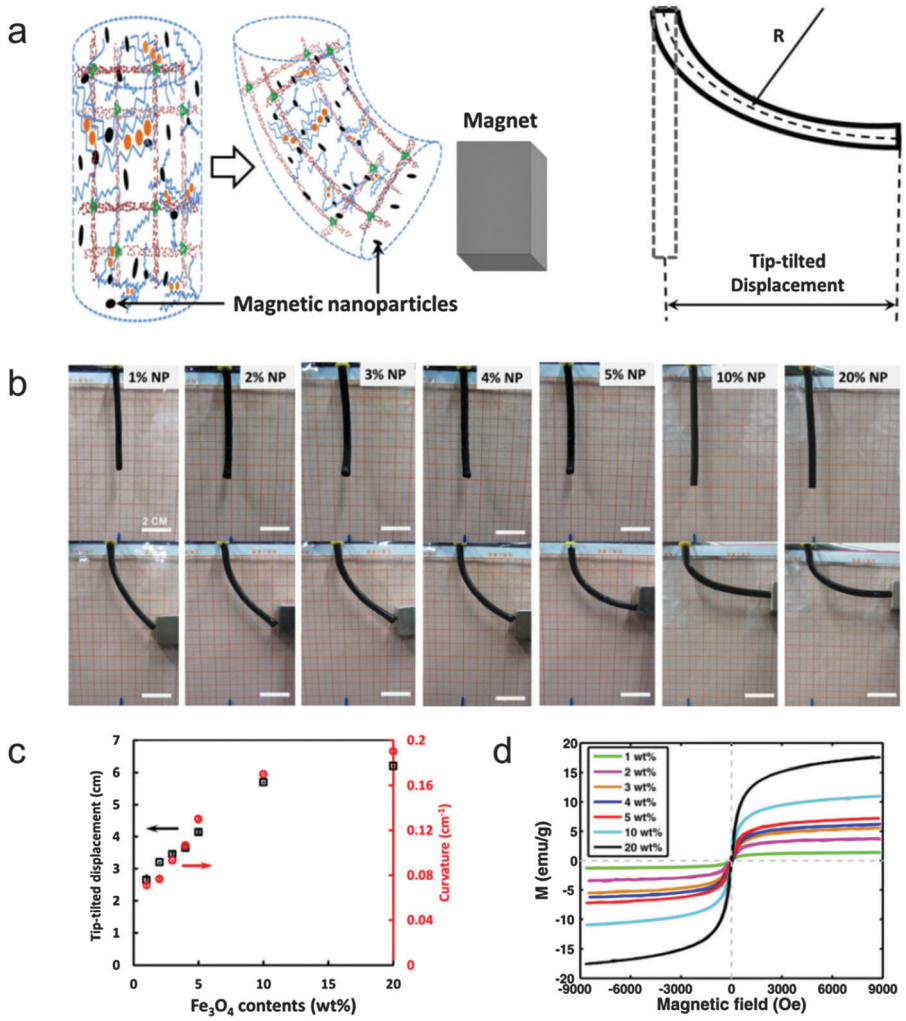

Fig. 5 A cantilever beam bending actuator made of the magnetic hydrogel. (a) Schematic of actuation, measurement of the tip-tilted displacement and curvature of the magnetic hydrogel under magnetic attraction. (b) Photographs of the responses of the magnetic hydrogels with varying content of Fe_3O_4 nanoparticles. Scale bars: 2 cm. (c) Tip-tilted displacement and curvature, and (d) magnetic hysteresis loops of the magnetic hydrogels. Error bars denote the standard deviation from at least three experiments.

at the point where the magnet detaches from the hydrogel. Both the tip-tilted displacement and curvature increase with increasing $W_{Fe_3O_4}$ as shown in Fig. 5b and summarized in Fig. 5c, which is as expected because the saturation magnetization increases with increasing $W_{Fe_3O_4}$ accordingly (Fig. 5d). As previously reported,[13] the maximum saturation magnetization of the magnetic hydrogels embedded with Fe_3O_4 nanoparticles exhibits a noticeable decline compared to that of the pure Fe_3O_4 nanoparticles, which is nearly 60 emu g^{-1} (ESI,† Fig. S3). The magnetic actuation performance can be enhanced if other nanoparticles with a higher saturation magnetization are embedded.[34] It is a challenge to balance the mechanical performance and magnetic properties of magnetic hydrogel nanocomposites. The higher the nanoparticle content, the better the magnetic properties of the hydrogel, whereas, in general, the stretchability and toughness are more limited.[35] In the case of our system, when the nanoparticle content reaches as high as 20 wt%, the mechanical performance of the magnetic hydrogel is lower than that of the magnetic hydrogels containing 1–10 wt% magnetic nanoparticles, but still higher than other reported magnetic hydrogels.[36]

3.4 Magnetically guided hydrogel catheter

The tough magnetic hydrogel holds great potential as a distal tip of a magnetic catheter or as a carrier of a magnetically guided capsule endoscope for clinical magnetic navigation systems. We first show the concept of a prototype guided magnetic catheter by using the magnetic hydrogel and a hydrogel tube as a model for soft tissues. A magnetic hydrogel cylinder was inserted into a transparent arc-shaped hydrogel tube made from a calcium ion crosslinked alginate/PAAm hydrogel (44.3 ± 1.9 kPa elastic modulus, 588.1 ± 62.4 kJ m^{-3} energy dissipation). The hydrogel tube can be used to mimic the environment of soft tissues, such as blood vessels and the intestinum. The navigation and maneuvering of the magnetic hydrogel was guided by a non-contact moving NdFeB alloy magnet. Fig. 6 presents the optical images of the magnetic

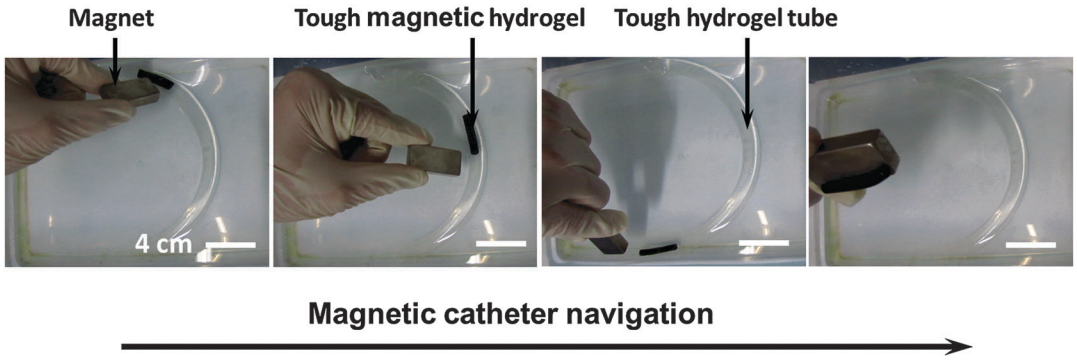

Fig. 6 Demonstration of the magnetic tough hydrogel catheter navigation. A cylindrically shaped magnetic hydrogel was inserted into a calcium ion crosslinked alginate/PAAm hydrogel tube. Both the magnetic hydrogel and the hydrogel tube were immersed in deionized water. A NdFeB magnet was use to remotely guide the magnetic hydrogel.

guidance and a recorded movie is given in Movie S4 (ESI†). When the NdFeB magnet was moved along the hydrogel tube, the magnetic hydrogel moved forward inside the tube under the guidance of the magnet. Finally, the magnetic hydrogel was navigated from one end of the tube to another, and attached to the magnet. The strong magnetic attraction and the low friction attributed to the smooth movement. Commercially, permanent magnets made of metal (magnet) or alloys (iron–cobalt alloy, NdFeB alloy) are used as distal tips of magnetic catheters or carriers of magnetically guided capsule endoscopes.[37,38] The advantages of replacing conventional stiff metal catheters or endoscope capsules by soft and wet magnetic hydrogels are obvious, as the friction between the catheter/capsule and soft tissues is reduced, avoiding potential hazards such as perforation or surgical bleed. These advantages are attributed to the softness and low friction of the magnetic hydrogel.[39]

4. Conclusions

Embedding magnetic nanoparticles into a hydrogel matrix results in magnetic hydrogels, which are soft, wet, and can be actuated in a non-invasive approach by a magnetic field with a fast response. Existing magnetic hydrogels, however, are weak and brittle, limiting their widespread applications. We developed a facile and versatile approach to fabricate tough and notch-insensitive magnetic hydrogels. This is realized by homogeneously incorporating Fe_3O_4 nanoparticles into a tough hydrogel with interpenetrated polymer networks. The magnetic hydrogels containing 1–20 wt% of alginate-coated Fe_3O_4 nanoparticles exhibit exceptional toughness, *e.g.*, 3–11 fracture strain, 200–1000 kPa tensile strength, 3.1–5.6 MPa compressive stress, and 1550–2800 J m^{-2} fracture energy. The toughness of the magnetic hydrogels is comparable to that of cartilage and rubber. In particular, even for the samples containing a pre-existing notch, a stretch to $\sim$9 times the original length without rupturing is achieved, demonstrating the notch-insensitivity of the developed magnetic hydrogel. A cantilever bending beam actuator and a prototype guided magnetic catheter demonstrate the potential applications of the magnetic hydrogels for soft robotics and clinical operations. Our approach is generic and can be adapted straightforwardly to other strong hydrogel systems and polymer composites. It is also easy to be scaled up for mass production. This opens up new opportunities to develop soft magnetic materials with exceptional mechanical properties and desirable functionalities for the advancement of new technology.

Acknowledgements

This research was supported by the National Natural Science Foundation of China (No. 51173144, 51073127, 11372239, 11472210, 31271023 and 11321062), the project of major research plan of the National Natural Science Fund of China (No. 91323104), International Science & Technology Cooperation Program supported by Ministry of Science and Technology of China and Shaanxi Province (2013KW14-02), the Research Fund for the Doctoral Program of Higher Education of China, the Scientific Research Foundation for the Returned Overseas Chinese Scholars, State Education Ministry, the Fundamental Research Funds for the Central Universities, the Program for the Key Science and Technology Innovative Team of Shaanxi Province (No. 2013KCT-05). The support of Collaborative Innovation Center of Suzhou Nano Science and Technology, Xi'an Jiaotong University is acknowledged. ZS acknowledges the support of NSF MRSEC (DMR-0820484) and visiting appointment at the International Center for Applied Mechanical.

References

1 G. Lattermann and M. Krekhova, *Macromol. Rapid Commun.*, 2006, **27**, 1373.
2 D. Szabo, I. C. Nagy, M. Zrinyi and A. Vertes, *J. Colloid Interface Sci.*, 2000, **221**, 166.
3 G. Lin, S. Chang, C.-H. Kuo, J. Magda and F. Solzbacher, *Sens. Actuators, B*, 2009, **136**, 186.
4 Y. M. Chen, Z. Q. Liu, Z. H. Feng, F. Xu and J. K. Liu, *J. Biomed. Mater. Res., Part A*, 2014, **102**, 2258.
5 Z. Wei, J. H. Yang, X. J. Du, F. Xu, M. Zrinyi, Y. Osada, F. Li and Y. M. Chen, *Macromol. Rapid Commun.*, 2013, **34**, 1464.
6 Z. Wei, J. H. Yang, J. Zhou, F. Xu, M. Zyrinyi, P. H. Dassault, Y. Osada and Y. M. Chen, *Chem. Soc. Rev.*, 2014, **43**, 8114.

7 Z. Liu, H. Wang, B. Li, C. Liu, Y. Jiang, G. Yu and X. Mu, *J. Mater. Chem.*, 2012, **22**, 15085.
8 R. Hernandez, V. Z. Mora, M. S. Ballestero, J. V. Baudrit, D. Lopez and C. Mijangos, *J. Colloid Interface Sci.*, 2009, **339**, 53.
9 R. Messing, N. Frickel, L. Belkoura, R. Strey, H. Rahn, S. Odenbach and A. Schmidt, *Macromolecules*, 2011, **44**, 2990.
10 Z. Varga, G. Filipcsei and M. Zrinyi, *Polymer*, 2006, **47**, 227.
11 Y. Li, G. Huang, X. Zhang, B. Li, Y. M. Chen, T. Lu, T. J. Lu and F. Xu, *Adv. Funct. Mater.*, 2013, **23**, 660.
12 F. Xu, C. M. Wu, V. Rengarajan, T. D. Finley, H. O. Keles, Y. Sung, B. Li, U. A. Gurkan and U. Demirci, *Adv. Mater.*, 2011, **23**, 4254.
13 Y. Zhou, N. Sharma, P. Deshmukh, R. K. Lakhman, M. Jain and R. M. Kasi, *J. Am. Chem. Soc.*, 2012, **134**, 1630.
14 Y. Gao, Z. Wei, F. Li, Z. M. Yang, Y. M. Chen, M. Zrinyi and Y. Osada, *Green Chem.*, 2014, **16**, 1255.
15 Y. Wang, A. Dong, Z. Yuan and D. Chen, *Colloids Surf., A*, 2012, **415**, 68.
16 S. Zhang, Y. Zhai and Z. Zhang, *Proceedings of the International Conference on Electronic and and Mechanical Engineering and Information Technology*, IEEE, Harbin, Heilongjiang, China, 2011.
17 C.-Y. Hui, A. Jagota, S. J. Bennison and J. D. Londono, *Proc. R. Soc. London, Ser. A*, 2003, **459**, 1489.
18 J. Qin, I. Aesmpah, S. Laurent, A. Fornara, R. N. Muller and M. Muhammed, *Adv. Mater.*, 2009, **21**, 1354.
19 Y. Zhang, Y. Sun, X. Yang, J. Hilborn, A. Heershap and D. A. Ossipov, *Macromol. Biosci.*, 2014, **14**, 1249.
20 L. L. Lao and R. V. Ramanujan, *J. Mater. Sci.:Mater. Med.*, 2004, **15**, 1061.
21 G. R. Souza, J. R. Molina, R. M. Raphael, M. G. Ozawa, D. J. Stark, C. S. Levin, L. F. Bronk, J. S. Ananta, J. Mandelin, M. M. Georgescu, J. A. Bankson, J. G. Gelovani, T. C. Killian, W. Arap and R. Pasqualini, *Nat. Nanotechnol.*, 2010, **5**, 291.
22 G. Bayramoglu, B. Altintas and M. Y. Arica, *Appl. Microbiol. Biotechnol.*, 2013, **97**, 1149.
23 C. H. Yang, M. X. Wang, H. Haider, J. H. Yang, J. Y. Sun, Y. M. Chen, J. Zhou and Z. Suo, *ACS Appl. Mater. Interfaces*, 2013, **5**, 10418.
24 T. W. Chung, J. Yang, T. Akaike, K. Y. Cho, J. W. Nah, S. I. Kim and C. S. Cho, *Biomaterials*, 2002, **23**, 2827.
25 Y. J. Heo, H. Shibata, T. Okitsu, T. Kawanishi and S. Takeuchi, *Proc. Natl. Acad. Sci. U. S. A.*, 2011, **108**, 13399.
26 H. Shibata, Y. J. Heo, T. Okitsu, Y. Matsunaga, T. Kawanishi and S. Takeuchi, *Proc. Natl. Acad. Sci. U. S. A.*, 2010, **107**, 17894.
27 N. A. Hadjiev and B. G. Amsden, *J. Controlled Release*, 2015, **199**, 10.
28 J. Buffle, Z. Zhanng and K. Startchev, *Environ. Sci. Technol.*, 2007, **41**, 7609.
29 M. Srivastava, J. Sing, M. Yashpal, D. K. Gupta, R. K. Mishra, S. Tripathi and A. K. Ojha, *Carbohydr. Polym.*, 2012, **89**, 821.
30 I. M. Sano, Y. Matsuda and H. Namiki, *Biomed. Mater.*, 2009, **4**, 025008.
31 N. K. Simha, C. S. Carlson and J. L. Lewis, *J. Mater. Sci.: Mater. Med.*, 2003, **14**, 631.
32 G. J. Lake, *Rubber Chem. Technol.*, 1995, **68**, 435.
33 J. Wu, X. Gong, Y. Fan and H. Xia, *Soft Matter*, 2011, **7**, 6205.
34 G. S. Chaubey, C. Barcena, N. Poudyal, C. Rong, J. Gao, S. Sun and J. P. Liu, *J. Am. Chem. Soc.*, 2007, **129**, 7214.
35 Y. Yang and M. W. Urban, *Chem. Soc. Rev.*, 2013, **42**, 7446.
36 S. Ghosh and T. Cai, *J. Phys. D: Appl. Phys.*, 2010, **43**, 415504.
37 L. Muller, M. Saeed, M. W. Wilson and S. W. Hetts, *J. Cardiovasc. Magn. Reson.*, 2012, **14**, 33.
38 P. Swain, A. Toor, F. Volke, J. Keller, J. Gerber, E. Rabinovitz and R. I. Rothstein, *Gastrointest. Endosc.*, 2010, **71**, 1290.
39 J. P. Gong, M. Higa, Y. Iwasaki, Y. Katsuyama and Y. Osada, *J. Phys. Chem. B*, 1997, **101**, 5487.